Nuclear Instruments and Methods in Physics Research B 281 (2012) 15–20

Contents lists available at SciVerse ScienceDirect

Nuclear Instruments and Methods in Physics Research B

journal homepage: www.elsevier.com/locate/nimb

How surface roughness affects the angular dependence of the sputtering yield

A. Hu *, A. Hassanein

Center for Materials under Extreme Environment, School of Nuclear Engineering, Purdue University, West Lafayette, IN 47906, USA

ARTICLE INFO

Article history:
Received 4 January 2012
Received in revised form 22 March 2012
Available online 2 April 2012

Keywords:
Angular sputtering
Roughness exponent
Random fractal
ITMC code

ABSTRACT

Comprehensive model is developed to study the impact of surface roughness on the angular dependence of sputtering yield. Instead of assuming surfaces to be flat or composed of exact self-similar fractals, we developed a new method to describe the surfaces. Random fractal surfaces generated by midpoint displacement algorithm in computer graphics area and Support vector machine algorithm in pattern recognition area are combined with the Monte Carlo ion bombardment simulation code, i.e., Ion Transport in Materials and Compounds (ITMC) code [1]. With this new fractal version of ITMC-F, we successfully simulated the angular dependence of sputtering yield for various ion-target combinations. Examples are given for 5 keV Ar ions bombarding iron, graphite, and silicon surfaces, with the input surface roughness exponent directly depicted from experimental data. Comparison is made with previous models to account for surface roughness and recent experimental data. The ITMC-F code showed good agreement with the experimental data.

1. Introduction

Materials sputtering yield from ion bombardment is by far one of the most commonly studied topics. In most previous related work, the bombarded surfaces are assumed to be flat and smooth in computer simulation or assumed to be exact self-similar fractals in analytical studies. However, both assumptions are not accurate enough to present the true material surfaces. In this research, we developed an innovative way to describe true surfaces.

In 1975, Benoît Mandelbrot introduced the concept of fractal based on the mathematical assumption of $(\text{line})^{\frac{1}{1}} = (\text{area})^{\frac{1}{2}} = (\text{volume})^{\frac{1}{3}}$, therefore if a rough surface has a dimension D greater than 2, then it should obey the modified relationship [2]:

$$(\text{area})^{\frac{1}{D}} = (\text{volume})^{\frac{1}{3}}$$

Based on this concept, numerous applications followed this idea for different research topics. In 1983, Peter Pfeifer along with David Avnir and Dina Farin used this concept for applications of measuring fractal dimension of material surfaces [3,4]. In their work, they used molecules adsorbed on material surface to determine surface roughness, and then used Brunauer–Emmett–Teller (BET) method and adsorption from hexane solution to measure the material surface area, where BET is a theory explains the physical adsorption of gas molecules on a material surface.

Later in 1990s, scientists started to use Scanning Tunneling Microscopy (STM) in experiments instead of gas adsorption techniques and the relation of average root-mean-square (rms) roughness versus scan size. The rms roughness of a surface is defined by:

$$\sigma = < [h(x,y) - h]^2 >^{\frac{1}{2}}, \quad (1)$$

where h is the average height.

The rms surface roughness increases with the sample length L following the relation $\sigma \propto L^H$. Here H is called the roughness exponent and has a value $0 < H < 1$, and relates to fractal dimension by $D = 3 - H$. Besides gas adsorption and STM, there are several other methods to determine surface roughness. These techniques include Atomic Force Microscopy (AFM), Reflection High-Energy Electron Diffraction (RHEED), High Resolution Low Energy Diffraction (HRLEED), Scanning Electron Microscopy (SEM), Transmission Electron Microscopy (TEM), as well as helium atom scattering have also been utilized.

In 1991, Eklund et al. exposed the (0001) surface of the highly-oriented pyrolytic graphite to 5 keV Ar+ ions at an angle of 60° with respect to substrate normal. After scanning the surface in STM, the roughness exponent for 300 K is determined to be 0.2–0.4 [5]. Another work is done in 1993 by Krim's group also using STM, they studied the erosion of Fe(100) films sputtered with 5 keV Ar+ ions at 300 K and obtained surface roughness exponent equals 0.53 ± 0.03 [6].

For more recent work, in 2003 Nath Dev's group used 2 MeV silicon ions bombarded on Si(100) surfaces (with native oxide) at room temperature with a fluence of 4×10^{15} ions/cm^2. In their research, ion-bombarded (IB) and ion-bombarded-thermally-treated (TIB) Si surfaces with native oxide have measured corresponding roughness exponents of 0.53 ± 0.03 and 0.81 ± 0.04, respectively

* Corresponding author. Tel.: +1 7654099162.
E-mail address: hu77@purdue.edu (A. Hu).

0168-583X/$ - see front matter © 2012 Elsevier B.V. All rights reserved.
http://dx.doi.org/10.1016/j.nimb.2012.03.026

[7]. Then in 2008, they used 45 keV silicon ions bombarded on Si(100) surfaces at room temperature with fluence of 4×10^{15} ions/cm^2, and observed a roughness exponent of 0.46 ± 0.04 [8], and the new result of 1 keV argon bombardment of silicon surface is found to have roughness exponent equals 0.23 ± 0.08 [9] by de Rooij-Lohmann et al.

In the simulations part, TRIM is a well-known binary-collision computer program for calculating material sputtering. However, material surface is assumed to be flat in TRIM to simplify the modeling, however in 1989, Ruzic added the fractal geometry into TRIM to model realistic surface roughness, and called this version VF-TRIM [10]. The rough surface he considered is composed by an exact self-similarity fractal. He also implemented the Snell's refraction law when an incident ion entering a surface [10], therefore the fraction relation between angle α and α':

$$\sin^2\alpha' = \frac{E_0}{E_0 + E_{sb}} \sin^2\alpha. \tag{2}$$

Where α is the initial incident angle and α' is the new angle. E_0 is the incident energy and E_{sb} is surface binding energy. This equation is actually the measure of refraction for a new particle hitting the surface. And from α' he can define the characteristic fractal dimension D:

$$D = \frac{\log\left(R\frac{P_{max}\tan\alpha' + P_{max}}{P_{max}/\cos\alpha'}\right)}{\log(R)} = \frac{\log(R(\cos\alpha' + \sin\alpha'))}{\log(R)} \tag{3}$$

This has the same form with the fractal dimension in the mathematical form:

$$D = -\lim_{r\to 0}\frac{\log N(r)}{\log r} \tag{4}$$

In 1998, Kustner et al. [11] also used TRIM in part of their simulation. They developed a model that uses a distribution of the local angles of ion incidence determined from STM measurement as well as the redeposition fraction to describe the fluence of the roughness on the yield. This distribution is used as input to TRIM to calculate the sputter yield of the target with the rough surface.

Another group lead by Albert-Laźló Baraśi had constructed an analytical model to implement the effects of surface roughness [12]. In their model, they considered single component systems and characterized the sputtering yield as a function of the roughness of self-affine surface and the primary ion penetration depth. They found in general, that the effect of the yield changes by the surface roughness is strongly dependent on the specifics of the surface roughness and the primary ion beam characteristics. In a certain range of parameters variations, the yield was found to decrease below the flat surface results, which means the surface roughness can both enhance and suppress the sputtering yields.

Yamamura group also added the fractal dimension parameter into their ACAT Monte Carlo simulation code [13]. They set the fractal dimension equals 2.1 to fit the experimental data. Incident 2 keV D+ ions bombarded Mo surface was simulated by the modified ACAT and compared to planar ACAT and experimental data.

In conclusion, there are numerous experimental and simulation research focused on surface roughness, but not yet a comprehensive integrated work is done to connect these two sides uniquely with realistic fractal dimension.

2. Model and methods

In the our simulation work, we use mid-point displacement algorithm to generate fractal Brownian motion in MATLAB with values of roughness exponents obtained from experimental results. Then we obtain sputtering yields from simulating ions bombardment on these surfaces.

2.1. Brownian motion and fractional Brownian motion

The Brownian motion can be viewed as a simplest continuous-time stochastic process. It has an expectation equals zero and the variance equals time. This continuous-time stochastic process is named after the mathematician Norbert Wiener. The Wiener process $W(t)$ is briefly characterized by three properties [14]:

(1) A Wiener process $W(t)$ for $t \geq 0$ has the property $W(0) = 0$.
(2) The function $t \to W(t)$ is almost surely continuous, where almost surely means the event happens with probability one in the probability theory.
(3) W_t has independent increments with

$$W(t) - W(s) \sim N(0, t-s) \text{ for } 0 \leq t. \tag{5}$$

Where $N(\mu, \sigma^2)$ denotes the normal distribution μ and variance σ^2. It has independent increments meaning that if

$$0 \leq s_1 < t_1 \leq s_2 < t_2. \tag{6}$$

Then $W(t_1) - W(s_1)$ and $W(t_2) - W(s_2)$ are independent random variables.

Fractional Brownian motion (fBm) was introduced by Mandelbrot and van Ness first in 1968. It is an extension of Brownian motion concept. It is still a continuous-time process which starts at zero. The difference between regular Brownian motion and fBm is that while the increments are independent Brownian motion, they are dependent in fBm by the covariance function [15]:

$$E[B^H(t)B^H(s)] = \frac{1}{2}(|t|^{2H} + |s|^{2H} - |t-s|^{2H}). \tag{7}$$

Assuming we have a fractional Brownian motion, $V_H(t)$, that is a single valued function of time. Then fBm can be characterized by a parameter H in the range $0 < H < 1$. H relates to

$$\Delta V = V(t_2) - V(t_1) \text{ and } \Delta t = t_2 - t_1 \text{ by } \Delta V \propto \Delta t^H. \tag{8}$$

The surface varies from roughest to relatively smooth while H varies from 0 to 1. In usual Brownian motion, the sum of increments is proportional to the square root of time, so when $H = \frac{1}{2}$ the trace corresponds to the usual Brownian motion. If $H > \frac{1}{2}$ then the increments of the process are positively correlated, and if $H < \frac{1}{2}$ then the increments of the process are negatively correlated. The fractal dimension definitions for fBm are $D = 2 - H$ for a fractal line and $D = 3 - H$ for a fractal landscape.

2.2. Midpoint displacement algorithm

Midpoint displacement algorithm is used to describe the fractional Brownian motion using the random Gaussian distribution in this model [15].

Consider the approximation to a simple fBm $V_H(t)$, where the mean square increment for points separated by a time $\Delta t = 1$ is σ^2. Then from $\Delta V \propto \Delta t^H$ for points separated by a time t:

$$< |V_H(t) - V_H(0)|^2 >= t^{2H} \cdot \sigma^2. \tag{9}$$

Here we assume $V_H(0) = 0$ and $t = \pm 1$ are Gaussian random variable with variance σ^2 to satisfy. Now we can define the midpoints value at $\pm\frac{1}{2}$ as:

$$V_H\left(\pm\frac{1}{2}\right) = 0.5[V_H(0) + V_H(\pm 1)] + \Delta_1, \tag{10}$$

where Δ_1 is a Gaussian random variable, and it has a mean equals zero and variance equals Δ_1^2.

From Eq. (10), we can see that

$$\Delta_1 = V_H\left(\pm\frac{1}{2}\right) - 0.5V_H(\pm 1), \tag{11}$$

because $V_H(0) = 0$.

Then from the variance formula:

$$Var(aX + bY) = a^2 Var(X) + b^2 Var(Y) + 2abCov(X, Y), \tag{12}$$

we can get

$$\Delta_1 = \frac{\sigma^2}{2^{2H}} - \frac{1}{4}var[\Delta H_1(1)] = \frac{\sigma^2}{2^{2H}}[1 - 2^{2H-2}]. \tag{13}$$

Where the covariance equals zero because the $V_H(\pm\frac{1}{2})$ and $V_H(\pm 1)$ are random variables that are uncorrelated. If we keep adding smaller stages:

$$V_H\left(\pm\frac{1}{4}\right) = 0.5[V_H(0) + V_H\left(\pm\frac{1}{2}\right)] + \Delta_2 \tag{14}$$

and the variance is

$$\Delta_2^2 = \frac{\sigma^2}{4^{2H}} - \frac{1}{4}var\left[\Delta H_1\left(\frac{1}{2}\right)\right] = \frac{\sigma^2}{4^{2H}}[1 - 2^{2H-2}]. \tag{15}$$

After several stages, we observe that there is a relation for each stage variance:

$$\Delta_n^2 = \frac{\sigma^2}{(2^n)^{2H}}[1 - 2^{2H-2}]. \tag{16}$$

However, this is not a stationary process. A stationary process in statistics means a stochastic process whose probability distribution will not change when shifted along time or space. As a result, points generated from different stages will have different statistical property from their neighbors. For example, although in fact the following equation is true

$$Var\left(X\left(\frac{1}{2}\right) - X(0)\right) = var\left(X(1) - X\left(\frac{1}{2}\right)\right) = \left(\frac{1}{2}\right)^{2H}\sigma^2, \tag{17}$$

however one cannot be sure that the variance will be the same for smaller stage point, in other word, we do not have the following relation

$$var\left(X\left(\frac{3}{4}\right) - X\left(\frac{1}{4}\right)\right) = \left(\frac{1}{2}\right)^{2H}\sigma^2. \tag{18}$$

In order to solve this problem, we need to use successive random addition. It means that after interpolating the midpoints, add displacements of a suitable variance to all of the points and not just the mid-points. We do this in the following steps:

1. Set the initial random corners which are the circle dots in the left graph.
2. Interpolate midpoints between corners, which are the square dots in the left graph in Fig. 1.
3. Add displacement to corner dots.
4. Rotate the left graph in Fig. 1 with 45°, which results the middle graph. Then interpolate boundary grid points between circle dots.
5. Interpolate interior grid points between square dots.
6. Add displacement to all points that exist before rotation then we got the right graph in Fig. 1.

However, a roughness exponent equal one does not mean the surface is totally smooth. As shown in Fig. 2, we can see that even $H = 1$, there is still some little waviness on the surface different from the flat assumption in ITMC [1].

2.3. Support vector machine

Since we use little grids to model the material surface, the surface itself is not a smooth function of position. Therefore, an important goal is how to find a plan that can represent the behavior of a small local region of a surface consisted by discrete particles other than simply differentiate the surface. Support vector machine (SVM) is a type of classification [16]. As shown in Fig. 3, it generates "separating hyperplane" to separate different data groups, and the plane which maximizes the distances from the hyperplane to the group margins is called "optimal separating hyperplane". In SVM, support hyperplanes mean the planes that are closest to the margin and parallel to the optimal separating hyperplane.

By using SVM algorithm, we can generate surface planes that well represent the local region character and determine the normal vector of the surface which can be used for the calculation of the surface energy barrier for the moving particle to rough surface. We can also calculate the reflection angles according to the plane generated from SVM when particles don't have enough energy to exit the surface and need to be reflected back to the material. Fig. 4 shows a 3∗3∗3 example of our simulation. The circles represent empty spots and the plus signs represent material particles on the surface, and the optimal separating hyperplane beautifully describes the character of this small region.

3. Results and discussion

To simulate the fractal effects, we used grid sizes $X = Y = Z = 5$ Å, and in total 128 grids for X and Y axes and 100 grids for Z axis, so the domain size for X and Y axes are 6.4×10^{-8} for Z axis is 5×10^{-8} cm.

Based on the work of Krim's group, the roughness exponent for the 5 keV argon ions bombarding the iron surface predicted $H = 0.53 \pm 0.03$ [6]. By using this value, we can construct a rough surface corresponding to their target and simulate the ion bombardment process with ITMC. The angular sputtering yield is shown in Fig. 5 in comparison to the original ITMC result and the

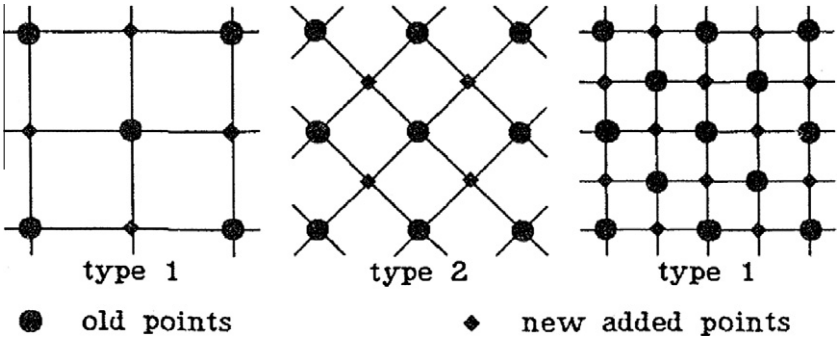

Fig. 1. Midpoint displacement steps [15].

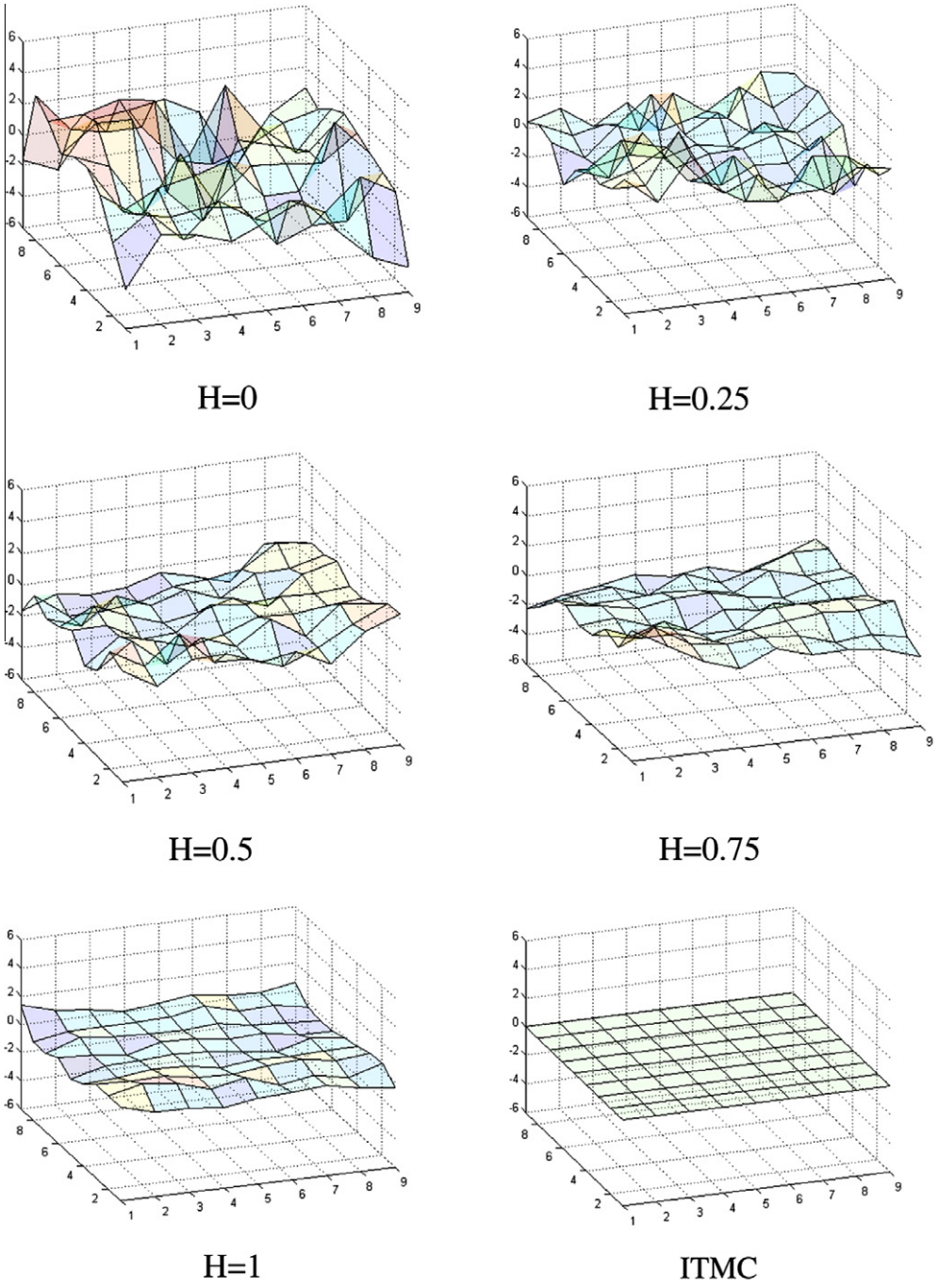

Fig. 2. Diagram with 9 by 9 surfaces having different roughness.

experiment data from Seah [17]. Good agreement is shown between ITMC-F and the data.

From the Eklund et al., the surface roughness exponent for graphite surface bombarded by 5 keV argon ions is predicted to be between 0.2 and 0.4 [5]. Therefore, we used roughness exponent equals 0.3 to construct the rough surface and obtain the angular sputtering yield and compared to experimental data and the original ITMC result. Fig. 6 shows again good agreement of ITMC-F with the data.

From the results of de Rooij-Lohmann et al. [9], the silicon surface was roughened with a 10 min, 1 keV argon ions bombardment at a grazing angle of 10° and the argon pressure is 1×10^{-3} mbar, and the surface ended up with a roughness exponent equals 0.23 ± 0.08. We used this value to construct the fractal surface and simulate the sputtering yield and compared to the experimental data and the original ITMC result. Fig. 7 also shows good agreement of ITMC-F with the data.

Similar trends in literature also confirm the validity of ITMC-F results by other simulation results when incorporating fractal roughness.

From the work of Ruzic shown in Fig. 8 [18], we can see that VFTRIM produced slightly higher sputtering yields compared to TRIM at small incident angle (about 0–40° range). While VFTRIM produced lower sputtering yield compared to TRIM at larger incident angle (about 40–85° range). Again TRIM assumes smooth material surface and VFTRIM assumes fractal surface.

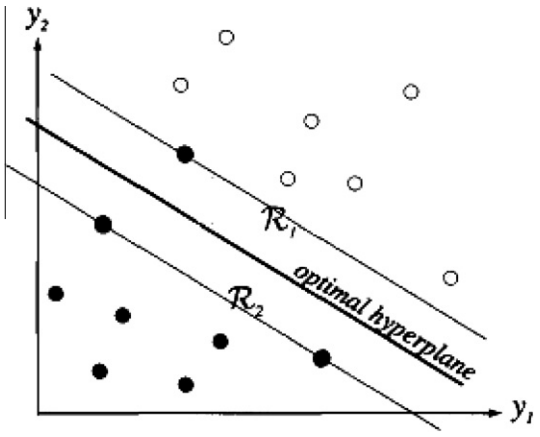

Fig. 3. Theorem of Support vector machine as discussed in [16].

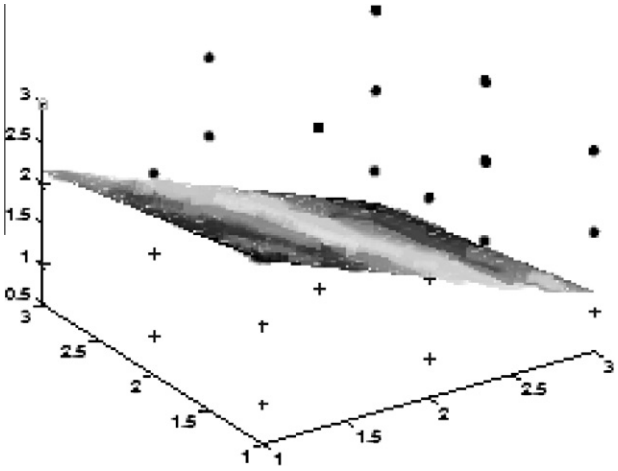

Fig. 4. Example of SVM on a 3∗3∗3 cube.

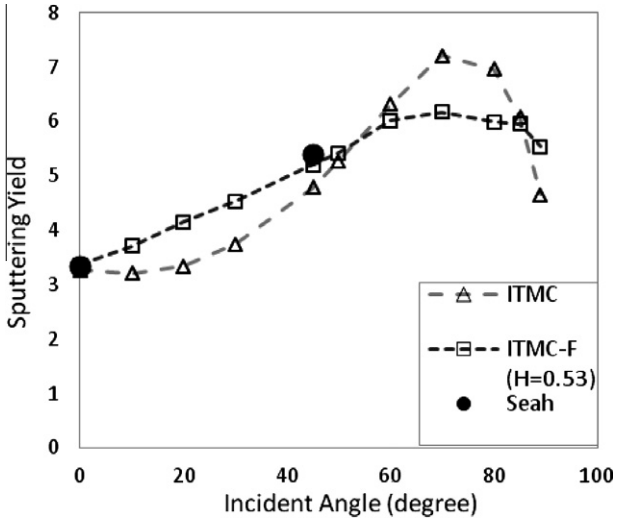

Fig. 5. Angular sputtering yield for 5 keV argon ions bombard on iron with $H = 0.53$ compared to ITMC and the experiment data.

The work of Kustner et al. [11] shown in Fig. 9 demonstrate the simulation of sputtering yield is lower than the prediction from a smooth surface at larger angles (about 50–85° range). While it is higher than the sputtering yield for smooth surface at smaller angles (about 0–50° range). The calculation for an atomically smooth graphite surface is shown as the solid line. The filled circles correspond to the calculations for rough surfaces and the filled squares represent the measured sputtering yields.

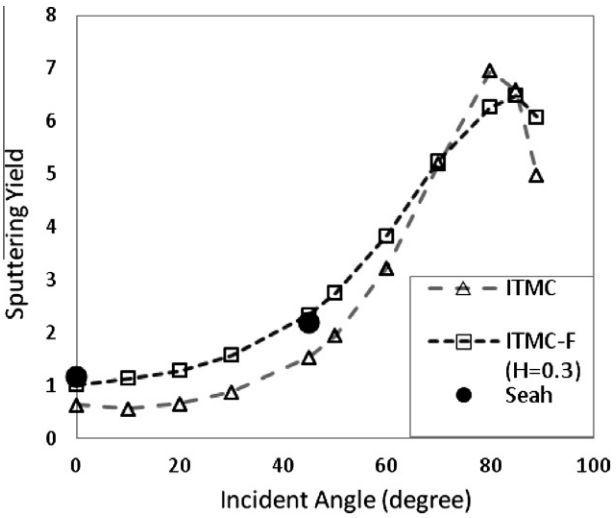

Fig. 6. Angular sputtering yield for 5 keV argon ions bombard on graphite with $H = 0.3$ compared to ITMC and experiment data.

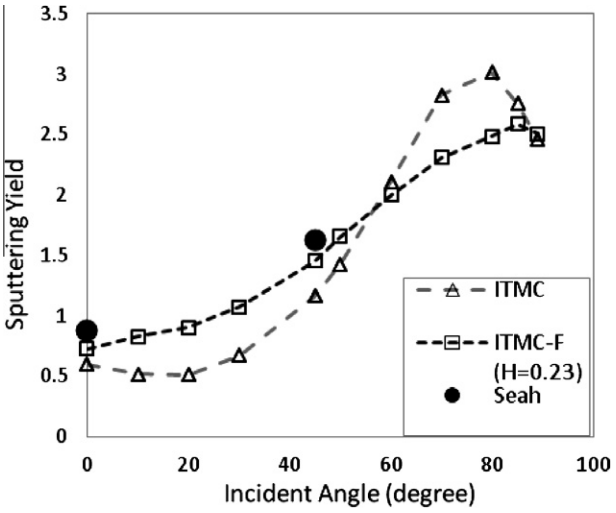

Fig. 7. Angular sputtering yield for 1 keV argon ions bombarded silicon with $H = 0.23$ compared to ITMC and the experimental data.

4. Conclusions

We developed a new method to describe rough surfaces and their effect on sputtering yields. Random fractal surfaces generated by midpoint displacement algorithm in computer graphics area and Support vector machine algorithm in pattern recognition area are combined with the Monte Carlo ion bombardment simulation code. The simulation code ITMC has been upgraded and added the new fractal dimension method in a new version of ITMC-F. We used the roughness exponent from available literature to decide the value of the fractal dimension we should use in simulating the material surfaces. As an example, we used $H = 0.53$ for 5 keV Ar ions bombard on iron, $H = 0.3$ for 5 keV Ar ions bombard on graphite and $H = 0.23$ for 1 keV Ar ions bombarding silicon to benchmark our ITMC-F code.

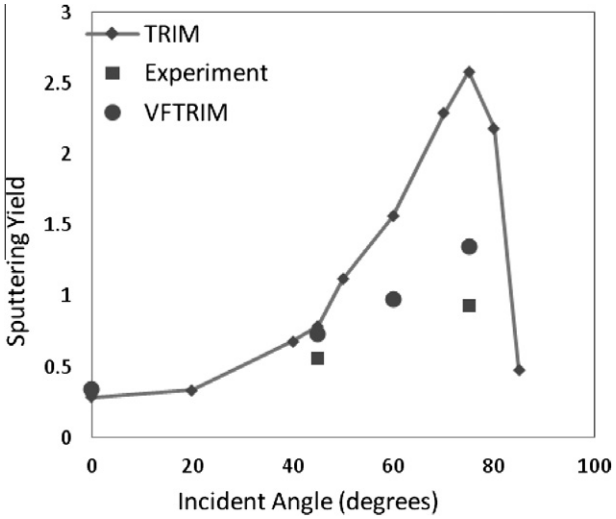

Fig. 8. VFTRIM data for the self sputtering of 1 keV Be as a function of incident angle with TRIM and experimental data.

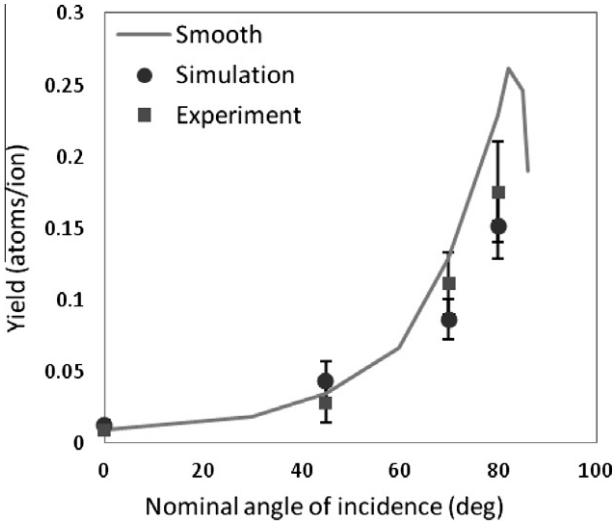

Fig. 9. Results from sputtering experiment for 2 keV *D* bombarding pyrolytic graphite are compared with calculations for sputter roughened pyrolytic graphite surfaces based on STM measurements.

We successfully simulated the angular dependence of sputtering yield for argon ions bombarding iron, graphite, and silicon surfaces, with incident angles varies from 0° to 89°. The results of ITMC-F code with roughness exponent assumption fit closer to the experimental data than original ITMC values. The trends of our results are also in agreement with other fractal surface simulations. By using this new developed model, we may be able to estimate the roughness exponent for material surfaces after ion bombardment in the future without doing experiments.

Acknowledgment

This work is supported by the US Department of Energy, Office of Fusion Energy Sciences.

References

[1] A. Hassanein, Fusion Technology 8 (1) (1985) 1735–1741.
[2] B.B. Mandelbrot, The Fractal Geometry of Nature, W.H. Freeman, 1982.
[3] P. Pfeifer, D. Avnir, Journal of Chemical Physics 79 (7) (1983) 3558–3565.
[4] D. Avnir, D. Farin, P. Pfeifer, Journal of Chemical Physics 79 (7) (1983) 3566–3571.
[5] E.A. Eklund et al., Physical Review Letters 67 (13) (1991) 1759–1762.
[6] J. Krim et al., Physical Review Letters 70 (1) (1993) 57–60.
[7] D.K. Goswami, B.N. Dev, Nuclear Instruments & Methods in Physics Research Section B-Beam Interactions with Materials and Atoms 212 (2003) 253–257.
[8] A. Roy et al., Nuclear Instruments & Methods in Physics Research Section B-Beam Interactions with Materials and Atoms 266 (8) (2008) 1276–1281.
[9] V.I.T.A. de Rooij-Lohmann et al., Applied Surface Science 256 (16) (2010) 5011–5014.
[10] D.N. Ruzic, Nuclear Instruments & Methods in Physics Research Section B-Beam Interactions with Materials and Atoms 47 (2) (1990) 118–125.
[11] M. Kustner et al., Nuclear Instruments & Methods in Physics Research Section B-Beam Interactions with Materials and Atoms 145 (3) (1998) 320–331.
[12] M.A. Makeev, A.L. Barabasi, Nuclear Instruments & Methods in Physics Research Section B-Beam Interactions with Materials and Atoms 222 (3–4) (2004) 316–334.
[13] T. Kenmotsu et al., Nuclear Instruments & Methods in Physics Research Section B-Beam Interactions with Materials and Atoms 228 (2005) 369–372.
[14] S.E.S. Ioannis Karatzas, Brownian Motion and Stochastic Calculus, second ed., Springer, 1991.
[15] C. Heinz-Otto Peitgen et al. (Eds.), The Science of Fractal Images, Springer-Verlag, 1988.
[16] P.E.H. Richard O. Duda, David G. Stork, Pattern Classification, second ed., Wiley, 2001.
[17] M.P. Seah et al., Surface and Interface Analysis 37 (5) (2005) 444–458.
[18] D.N. Ruzic, P.C. Smith, R.B. Turkot, Journal of Nuclear Materials 241 (1997) 1170–1174.